Metrologia 10, 87—98 (1974)
© by Springer-Verlag 1974

Determination of Velocity Distributions in Molecular Beam Frequency Standards from Measured Resonance Curves

Stephen Jarvis, Jr.

National Bureau of Standards, Boulder, Colo. 80302, USA

Abstract

It is shown that the Ramsey resonance curves for most atomic beam machines can be conceived as depending on two distributions of velocity, $\varrho\,(V)$ and $\xi\,(V)$, the second being a correction for beam width.

An analysis and computer program are described which permit one to obtain ϱ, ξ and the nominal microwave power parameter from three or more measured Ramsey resonance curves at properly spaced power levels whose ratios are known. The determination from the functions (ϱ, ξ) of bias errors due to second order Doppler shift, cavity phase difference, and cavity pulling is described.

The method may also be used to improve an experimentally obtained velocity distribution (i.e., one obtained through the pulse technique); to provide the proper function ξ; and to provide diagnostic checks of the measurement technique and the validity of the model chosen for the transition probability.

The method is applied to the NBS frequency standard. Error estimates indicate that it is feasible by microwave power shift measurements to evaluate the total bias error due to the above sources to within one part in 10^{13}.

I. Introduction

This paper deals with aspects of accuracy evaluation of molecular beam frequency standards of Ramsey type. Sources of error in the accuracy of such standards have been discussed by several authors [1—6]. For the high precision standards with which we shall specifically deal, the largest uncertainties, with which this paper is concerned, are in the errors caused by the cavity phase difference δ between the second and the first resonant cavity fields, and the second-order Doppler shift (DS) due to the difference

$$\nu_x - \nu = -\nu_x \frac{V^2}{2c^2}$$

between the laboratory-measured frequency ν_x in the cavities and the driving frequency ν experienced by the atoms with velocity V.

The bias, or accuracy error, due to DS and δ, as well as δ itself, can be estimated with sufficiently high precision to be acceptable in state-of-the-art frequency standards only from a rather good knowledge of the velocity distribution $\varrho\,(V)$ of the detected atoms in the particular mode of operation. Furthermore, while the bias due to DS can be computed directly from $\varrho(V)$, the bias due to δ, as well as δ itself, necessarily involves an accurate measurement of the resonant frequency shift between two operating modes (e.g., two power levels, beam reversal, or narrow-band velocity filtering), from which δ and its associated bias can be determined from the velocity distributions associated with the two modes.

The paper deals largely with the determination of $\varrho\,(V)$, and its use in the estimation of δ and DS based on power shift measurements.

An experimental method has recently been reported [7] which permits direct determination of the velocity distribution $\varrho\,(V)$ of detected atoms. Rf power is applied to the cavity in short pulses of length τ at a frequency ν_p. Those atoms which are driven in both cavities and generate a Ramsey resonance component in the detected signal are those whose time of flight T_f between the cavities is close to $1/\nu_p$. Since

$$T_f = \frac{L}{V} = \frac{n}{\nu_p}, \quad (n = 1, 2, \ldots),$$

fixing ν_p selects for detection those atoms whose velocities are close to

$$\nu_p L\,,\ \tfrac{1}{2}\nu_p L\,, \ldots$$

This multiplicity in n is a minor problem in precision beam standards for which the velocity distributions are typically rather narrow. A somewhat more difficult problem is presented by the window width ΔV around V of contributing atoms due to the finite cavity width and the finite pulse length τ, so that the distribution $\varrho_x\,(V)$ obtained by this method is actually a mean of the true distribution over the window ΔV. The methods described in this paper can make use of $\varrho_x\,(V)$ obtained by this experimental method to obtain more precise estimates of $\varrho\,(V)$.

If the window width ΔV is negligible, the pulse method leads to the interrogation of monovelocity beams, for which the bias due to DS is immediately known. The cavity phase difference δ and its associated bias are easily obtained from a measurement of the resonance shift between two selected velocities (two pulse frequencies ν_p). For non-negligible window widths ΔV, these results can be corrected for the windowing effect from a knowledge of $\varrho\,(V)$.

In Section II (A), the determination of Ramsey resonance patterns $g_x\,(\lambda, b)$ obtained from known beam optics, δ, and power parameter b is described. The effect of beam optics is shown to be describable in terms of two functions of velocity, $[\varrho\,(V),\ \xi\,(V)]$. In Section II (B), we assume that the distributions $[\varrho\,(V),\ \xi\,(V)]$ are known either by pulse technique measurements or by the analytical techniques of Section III. The problem of determining δ and the biases due to δ and DS from power shift measurements is reduced to the calculation of two mean velocities (V_D, V_p) and the determination of the power parameters used. The velocities (V_D, V_p) depend on the functions $[\varrho\,(V), \xi\,(V)]$, the cavity power parameter b, and the

frequency modulation width ν_M and mode (square wave, sinusoidal) used to determine the center of the Ramsey resonance peak. The bias due to cavity pulling is shown to depend on a third mean velocity V_B.

Section III describes an analysis and computer program for the determination of $[\varrho(V), \xi(V), b]$ from a set of Ramsey resonance curves taken at different power levels whose ratios are known. The method can be used for an independent determination of these quantities, for controlled improvement of experimental determinations of these quantities, and as a diagnostic test of the assumptions involved in the theory used in Section II.

Section IV describes the application of these methods to the accuracy evaluation of the NBS frequency standard NBS-5.

II. Theoretical Background

A. Ramsey Resonance Curve and the Velocity Distribution

In an atomic beam frequency standard of Ramsey type, with cavities No. 1 and No. 2 separated by a distance L, an atom with velocity V which sees field strength parameters (b_1, b_2) in the two cavities at driving frequency ν has a probability of changing state (transition probability) [6]

$$P(\lambda, V, b_1, b_2, \delta)$$

where $\lambda \equiv 2\pi(\nu - \nu_0)$ (this has the opposite sign from Ramsey's usage), ν_0 is the atomic resonance frequency, and δ is the phase lead of the second cavity over the first. When the field strength parameters differ little from each other and from a common value b over the portions of the resonant cavities traversed by the detected atoms, we write

$$b_i = b(1 - \epsilon_i), \qquad |\epsilon_i| \ll 1, i = 1, 2. \tag{2.1}$$

The transition probability assumes the form (see Appendix)

$$P(\lambda, V, b_1, b_2, \delta) = P_0(\lambda, V, b, \delta) - (\epsilon_1 + \epsilon_2) P_\epsilon(\lambda, V, b, \delta) \tag{2.2}$$

to the first order in the ϵ_i, when

$$P_0(\lambda, V, b, \delta) = \tfrac{1}{8}\sum_{q=1}^{8} K_q(\lambda, b) \cos\left(\frac{L_q}{V} + \mu_q\delta\right)$$

$$P_\epsilon(\lambda, V, b, \delta) = \tfrac{1}{8}\sum_{q=1}^{8} M_q(\lambda, b) \cos\left(\frac{L_q}{V} + \mu_q\delta\right) + N_q(\lambda, b) \sin\left(\frac{L_q}{V} + \mu_q\delta\right) \tag{2.3}$$

The first of these is equivalent to Ramsey's equation V. 44, [6]. The coefficients $K_q, L_q, M_q, N_q, \mu_q$ are given in Table 1; l is the effective width of each resonant cavity.

When $\frac{\lambda}{b} \ll 1$ in each cavity, i.e., near resonance, Eq. (2.3) reduce to the simpler form

$$P_0(\lambda, V, b, \delta) = 2\sin^2\left(\frac{2lb}{V}\right)\cos^2\tfrac{1}{2}\left(\frac{\lambda L}{V} + \delta\right)$$

$$P_\epsilon(\lambda, V, b, \delta) = \left(\frac{2lb}{V}\right)\sin\left(\frac{4lb}{V}\right)\cos^2\tfrac{1}{2}\left(\frac{\lambda L}{V} + \delta\right) \tag{2.4}$$

In most beam tubes, due to precise mechanical and electrical adjustment, δ is small (milliradians), the second order Doppler shift is small (ν is close to the laboratory driving frequency ν_x), and the cavity windows, centered on a field maximum, are small enough that the ϵ_i are small for all rays that reach the detector. Then with regard to the resonance patterns experimentally measured, $g_x(\lambda_x, b)$, where $\lambda_x = 2\pi(\nu_x - \nu_0)$, we may neglect the phase δ, and replace λ_x by λ in Eq. (2.2). We shall retain the first order terms in ϵ_i.

The detectable beam is usually quite narrow, so that all detected atoms may be considered to have been emitted with the same oven velocity distribution $\varrho_M(V)$. But as a result of beam optics and interfering surfaces, those emitted from different points on the emitter at different angles will be detected only for very different velocity ranges. Let $\vec{p}$ be a parameter vector denoting position and angular coordinates of launch of atoms from the emitter face. For each velocity V, we must distinguish four trajectory types which may reach the detector: for atoms in a given state j ($j = 1, 2$, depending on the sign of the magnetic moment), there are those ($k = 1$) that reach the detector only if transition occurs between the deflecting magnets (probability P), and those ($k = 2$) that reach the detector only if transition does not occur (probability $(1 - P)$. Atoms which reach the detector in either case or neither case generate a background signal independent of λ, and can be ignored. (They do, of course, affect stability by generating additional shot noise). We shall assume that the detected current $g_D(\lambda_x, b)$ is the same as the measured Ramsey resonance curve $g_x(\lambda_x, b)$ to within a scale factor $s(b)$ and a baseline shift $c(b)$.

For each velocity V, and for each (j, k), there is a $\vec{p}$-domain $\mathscr{R}^{jk}(V)$ of ray source parameters for detectable rays. The atoms reaching the detector then generate the current:

$$g_D(\lambda, b) = \int_0^\infty dV\, \varrho_M(V) \cdot \sum_{j=1}^{2} \cdot \left\{ \int_{\mathscr{R}^{j1}(V)} d\vec{p}\, P(\lambda, V, b_1(\vec{p}, V), b_2(\vec{p}, V), \delta) + \int_{\mathscr{R}^{j2}(V)} d\vec{p}\, [1 - P(\lambda, V, b_1(\vec{p}, V), b_2(\vec{p}, V), \delta)] \right\} \tag{2.5}$$

Ignoring the λ-independent term (unity) in the last integral, and letting $Q^{jk}(\vec{p}, V)$ be a support function on $\mathscr{R}^{jk}(V)$, ($Q^{jk} = 1$ if $\vec{p} \in \mathscr{R}^{jk}$, 0 otherwise):

$$g_D(\lambda, b) = \int_0^\infty dV\, \varrho_M(V) \left[\int d\vec{p}\, Q^*(\vec{p}, V) \cdot P(\lambda, V, b_1(\vec{p}, V), b_2(\vec{p}, V), \delta)\right] \tag{2.6}$$

where

$$Q^*(\vec{p}, V) = \sum_{j=1}^{2} [Q^{j1}(\vec{p}, V) - Q^{j2}(\vec{p}, V)]. \tag{2.7}$$

Then from Eq. (2.2), with $\epsilon(\vec{p}, V) = \epsilon_1(\vec{p}, V) + \epsilon_2(\vec{p}, V)$, we obtain from (2.6):

$$g_D(\lambda, b) = \int_0^\infty dV \{\varrho_M(V)\, q_0(V)\, P_0(\lambda, V, b, \delta) - \varrho_M(V)\, q_\epsilon(V)\, P_\epsilon(\lambda, V, b, \delta)\} \tag{2.8}$$

where:

$$q_0(V) = \int d\vec{p}\, Q^*(\vec{p}, V) \tag{2.9}$$

$$q_\epsilon(V) = \int d\vec{p}\, Q^*(\vec{p}, V)\, \epsilon(\vec{p}, V). \tag{2.10}$$

These latter integrals, over the region $\mathscr{R}(V, \vec{p})$ of detectable rays, may be calculated from "ray-tracing" techniques (i.e., studies of the trajectories of the atoms) if the magnetic field and geometric structure of the beam machine are adequately known.

Defining then the two velocity "distributions" of detected atoms:

$$\varrho(V) = \varrho_M(V)\, q_0(V)\,, \qquad (2.11)$$
$$\xi(V) = \varrho_M(V)\, q_\in(V)\,,$$

the measured Ramsey resonance curve, to within scaling factors s (b), c (b), must be:

$$s(b)\, g_x(\lambda_x, b) + c(b) = \int_0^\infty dV \{\varrho(V) P_0(\lambda, V, b, \delta) - \xi(V) P_\in(\lambda, V, b, \delta)\}\,. \qquad (2.12)$$

It should be noted from this development that the addition of a (small) constant $c_0 \cdot$ to ϵ_i can be absorbed as a multiplicative factor on b and ϵ_i; referring to (2.1),

$$b(1-(\epsilon_i + c_0)) = [(1-c_0)\, b]\left[1 - \frac{\epsilon_i}{1-c_0}\right] \equiv b^1(1-\epsilon_i^1)\,.$$

We may then fix a scale for the parameter b by requiring:

$$\int_0^\infty dV\, \xi(V) = 0\,. \qquad (2.13)$$

It should be noted further that, from Eq. (2.7), Q^* may be negative if $k=2$ type atoms exceed $k=1$ type for some velocity V. This could lead to negative values for $\varrho(V)$, but none have yet been experimentally determined or resulted from the techniques of Section III. The assumption $\varrho_M(V)$ independent of ray could easily be dropped by including $\varrho_M(V, \vec{p})$ in the integrals (2.9, 2.10); the result of this paper is unaffected. The present approach permits identification with on-going ray trace studies, which determine $q_0, q_\in$.

In Section III, Eq. (2.12) is used as the starting point in a method described for determining the velocity distributions $[\varrho(V), \xi(V)]$ from Ramsey resonance curves measured at power parameter settings (b_1, b_2, b_3) for which the ratios b_1/b_2 and b_1/b_3 are known.

B. Bias Errors for Sinusoidal and Squarewave Frequency Modulation

The center of the resonance curve $g_x(\lambda_x, b)$, may be located experimentally with very high precision by (slow) square-wave or sinusoidal modulation of the laboratory driving frequency ν_x and servo techniques based on the assumption that $g_D(\lambda_x, b)$ is symmetric about the peak. Thus it is essential to know how far removed this peak is from the atomic resonance ν_0.

Because of the DS effect, the cavity frequency ν seen by atoms with velocity V differs from the laboratory measured frequency:

$$\nu = \nu_x\left(1 + \frac{V^2}{2c^2}\right).$$

Since ν_x is very close to the atomic resonance over the Ramsey resonance curve $\lambda/2b \ll 1$, this can be written:

$$\nu = \nu_x + V^2\psi\,, \quad \psi \equiv \frac{\nu_0}{2c^2}\,. \qquad (2.14)$$

In the modulation method, $\nu_x(t)$ is fixed to be a center frequency ν_c on which is superposed a periodic frequency $\nu_M(t)$, which is very symmetric:

$$\nu_M(t) = -\nu_M\left(t + \frac{T}{2}\right)$$

where T is the modulation period. Thus:

$$\nu(t) = \nu_c + \nu_M(t) + V^2\psi\,. \qquad (2.15)$$

The detector current, $G_D(t, \nu_c)$, reflecting this modulation, is fed into a linear filter $\mathscr{L}$ designed to produce a null output when ν_c is adjusted to make:

$$G_D\left(t + \frac{T}{2}, \nu_c\right) = G_D(t, \nu_c)\,.$$

For squarewave modulation (SQ),

$$\nu_M(t) = \begin{cases} \nu_{M^\circ}, \text{ first half-cycle} \\ -\nu_{M^\circ}, \text{ second half-cycle} \end{cases}$$

and $\mathscr{L}_{SQ}$ forms a time-average of the difference

$$G_D\left(t + \frac{T}{2}, \nu_c\right) - G_D(t, \nu_c)\,.$$

For sinusoidal modulation (SS),

$$\nu_M(t) = \nu_{M^\circ} \sin \Omega t, \Omega = 2\pi/T\,,$$

and $\mathscr{L}_{SS}$ generates a time-average second-harmonic amplitude:

$$\int_0^T dt \sin \Omega t\, G_D(t, \nu_c)\,.$$

We shall assume that ν_M satisfies the condition $\frac{2\pi\nu_M}{b} \ll 1$, and use the simplified form, Eq. (2.4), for the transition probability to define P_0, $P_\in$ of Eq. (2.8). Then defining:

$$\varrho^*(V, b) \equiv \varrho(V)\left(1 - \cos\frac{4lb}{V}\right) - \frac{2lb}{V}\xi(V)\sin\frac{4lb}{V}$$
$$\Delta \equiv \nu_c - \nu_0 \qquad (2.16)$$

we may expand $G_D(t)$ to first order in the small quantities (Δ, ψ, δ):

$$G_D(t, \nu_c) = \int_0^\infty dV\, \varrho^*(V, b) \cos^2 1/2 \left[\frac{2\pi L}{V}(\Delta + \psi V^2 + \nu_M(t)) + \delta\right]$$
$$= \int_0^\infty dV\, \varrho^*(V, b) \cos^2\left(\frac{\pi L \nu_M(t)}{V}\right) - \pi L \int_0^\infty dV\, \varrho^*(V, b) \sin\left(\frac{2\pi L \nu_M(t)}{V}\right)\left[\frac{\Delta}{V} + V\psi + \frac{\delta}{2\pi L}\right].$$

After $\mathscr{L}$-filtering, the first term vanishes, while filtering of the second term gives an expression for the offset Δ:

$$\Delta(b, \nu_{M^\circ}) = \nu_c - \nu_0 = -\frac{\nu_0}{2c^2} V^2{}_D - \frac{\delta}{2\pi L} V_p \qquad (2.17)$$

where:

$$V^2{}_D(b, \nu_{M^\circ}) \equiv \frac{\langle V\rangle}{\left\langle\frac{1}{V}\right\rangle} \qquad (2.18)$$

$$V_p(b, \nu_{M^\circ}) \equiv \frac{\langle 1\rangle}{\left\langle\frac{1}{V}\right\rangle}$$

and

$$\langle F(V)\rangle \equiv \int_0^\infty dV\, \varrho^*(V, b)\, F(V)\, \mathscr{L}\left\{\sin\frac{2\pi L \nu_M(t)}{V}\right\}. \qquad (2.19)$$

For squarewave modulation, we have:

$$\langle V^m \rangle = 2 \int_0^\infty dV\, \varrho^* (V, b)\, V^m \sin \frac{2\pi L \nu_{M^\circ}}{V} . \tag{2.20}$$

For sinusoidal modulation, we have:

$$\langle V^m \rangle = 2 \int_0^\infty dV\, \varrho^* (V, b)\, V^m \Phi_p (V, \nu_M),$$

$$\Phi_p (V, \nu_{M^\circ}) \equiv \frac{1}{T} \int_0^\infty dt \sin \Omega t \sin \left(\frac{2\pi L \nu_{M^\circ}}{V} \sin \Omega t \right)$$

$$= J_1 \left(\frac{2\pi L \nu_{M^\circ}}{V} \right) \tag{2.21}$$

in terms of the Bessel function $J_1 (z)$.

The presentation so far given lends itself easily to the inclusion of cavity-pulling error. We assume the cavity power parameter b used in the development is related to an external power parameter b_x

$$b = b_x (1 - \mathscr{B} \lambda)$$

to within an undetermined scale factor with $|\mathscr{B} \lambda| \ll 1$ over the Ramsey resonance. The parameter $\mathscr{B}$ has the form:

$$\mathscr{B} = \frac{Q^2_{cav} (\nu_0 - \nu_{cav}) 2\pi}{1 + Q^2_{cav} (\nu_0 - \nu_{cav}) 2\pi}$$

where ν_{cav} is the cavity resonant frequency, Q_{cav} the cavity Q. To first order, Eq. (2.1) is

$$b_t = b_x (1 - \epsilon_t - \mathscr{B} \lambda) . \tag{2.22}$$

Then in Eq. (2.8), we replace $q_\epsilon (V)$ by $q_\epsilon (V) + 2 b\lambda \vec{p}\, q_0 (V)$. Noting that $\mathscr{B} \lambda$ is independent of $\vec{p}$, the preceding calculation gives for (2.17) the extended form

$$\Delta (b, \nu_{M^\circ}) \equiv \nu_c - \nu_0$$

$$= -\frac{\nu_0}{2c^2} V^2_D - \frac{\delta}{2\pi L} V_p - \frac{\mathscr{B} \nu_{M^\circ}}{2\pi L} V_B \tag{2.23}$$

where

$$V_B (b, \nu_{M^\circ}) = \frac{16\pi b l \int_0^\infty dV \varrho(V)\, \Phi_B (V, \nu_{M^\circ}) \dfrac{\sin \left(\frac{4bl}{V} \right)}{V}}{\left\langle \frac{V}{1} \right\rangle}$$

with

$$\Phi_B \equiv \mathscr{L} \left\{ \frac{\nu_M (t)}{\nu_{M^\circ}} \cos^2 \frac{\pi L \nu_M (t)}{V} \right\}$$

For squarewave modulation:

$$\Phi_B = 2 \cos^2 \left(\frac{\pi L \nu_{M^\circ}}{V} \right)$$

For sinusoidal modulation:

$$\Phi_B = \frac{1}{T} \int_0^T dt \sin^2 \Omega t \cos^2 \left(\frac{\pi L \nu_{M^\circ}}{V} \sin \Omega t \right)$$

$$= \frac{1}{2} \left[\frac{1}{2} - \frac{V}{2\pi L \nu_{M^\circ}} J_1 \left(\frac{2\pi L \nu_{M^\circ}}{V} \right) + J_0 \left(\frac{2\pi L \nu_{M^\circ}}{V} \right) \right]$$

Once velocity distributions $[\varrho (V), \xi (V)]$ are known, the coefficients $[V_D (b, \nu_{M^\circ}), V_P, V_B (b, \nu_{M^\circ})]$ for the bias [Eq. (2.17)] are easily computed by numerical integration.

If the bias shift $(\nu^1_c - \nu^2_c)$ between two different power levels (or two modulation widths) is measured experimentally, Eq. (2.17) [or (2.23) if cavity-pulling is significant and $\mathscr{B}$ is known) can be used to determine the phase shift δ, and hence the bias of each of the center frequencies ν^1_c and ν^2_c, and the bias at any other power level for which the ratio b/b_1 is known.

III. Analytical Determination of Velocity Distributions from Resonance Curves

In this section we shall describe an analysis and computer program which can be used to determine the distributions $[\varrho (V), \xi (V)]$ and the power parameter b from measured Ramsey resonance curves only. This amounts essentially to inversion of Eq. (2.12) considered as a Fredholm integral equation of the first kind with an unkhown parameter b.

The purpose of such a program is threefold. First, in the absence of a $\varrho_x (V)$ experimentally determined [$\xi (V)$ cannot be measured], the program provides both $\varrho (V)$ and $\xi (V)$ with very little ambiguity when resonance curves are carefully recorded at three or more power levels whose ratios are carefully set and which are sufficiently distinct: for example, near optimum power, and above and below this level by a few dB.

Second, if a measured distribution $\varrho_x (V)$ is available, the program can be used to improve the accuracy of $\varrho_x (V)$, determining $\xi (V)$ and a nominal value of b (assuming l is known), and provide a critical diagnosis of the measurement procedure.

Third, it provides a check on the validity of the model chosen for the transition probability. That is, if $[\varrho (V), \xi (V)]$ cannot be found to fit the resonance curves to whithin acceptable limits, one must suspect the presence of spectral impurities, extraneous transitions, microwave leakage into the drift region or some other problem. Such a result would put in doubt biases estimated from the simple transition probability and any velocity distribution.

Because $U = 1/V$ is the natural variable in the oscillating functions of the transition probability and in (uniform field) ray-tracing, we have defined:

$$V^2 \varrho (V) = R (U)$$
$$V^2 \xi (V) = E (U) \tag{3.1}$$

and written the integral in Eq. (2.12) in the form:

$$s (b)\, g_x (\lambda, b) + c (b)$$
$$= \int_{U_H}^{U_L} dU \, [R (U)\, P_0 (\lambda, V, b, 0) - E (U)\, P_\epsilon (\lambda, V, b, 0)] \tag{3.2}$$

neglecting the cavity phase shift δ and the second order Doppler shift $\nu - \nu_x$. Here $U_L = \frac{1}{V_L}$ and $U_H = \frac{1}{V_H}$ are given cutoffs to be determined by trial-and-error. (Estimates can be provided by ray-tracing, partial or complete measurements of $\varrho_x (V)$, or by judicious guessing).

For chosen N_0, setting $U_0 \equiv U_L$ and $U_{N_0+1} \equiv U_H$, we set at equal intervals h in U:

$$(U_0, U_1, \ldots, U_{N_0}, U_{N_0+1})$$

discrete values, and assume $R (U)$ and $E (U)$ vanish at the endpoints. Interpolating $R (U)$ and $E (U)$ by second-order spline functions (with minimum rms second derivative), we do the integrals exactly, so that we obtain the forms:

$$s\,(b)\,g_x\,(\lambda, b) + c\,(b) = \sum_{i=1}^{N_0} R_i\,P_i\,(\lambda, b) + E_i\,Q_i\,(\lambda, b) \tag{3.3}$$

with known (P_i, Q_i), unknown (R_i, E_i).

We also discretize λ:

$$\lambda_1 = 0, \lambda_m = (m-1)\,\lambda^*, \quad (m = 1, M)\,,$$

in equal steps λ^* spanning the major portion of the Ramsey resonance. Given Ramsey data $\{g_x\,(\lambda_\alpha, B^\beta\,b), \alpha = 1, N_\alpha\}$ for $\beta = 1, \ldots, N_\beta$ are interpolated quadratically over $\{\lambda_m\}$; we assume the ratios $B^\beta = \frac{b^\beta}{b}$ are given. Then in an obvious notation, Eq. (3.3) takes the discrete form:

$$s^\beta\,g_x^{m\beta} + c^\beta = g_0^{m\beta}$$

$$g_0^{m\beta} = \sum_{i=1}^{N_0} R_i\,P_i^{m\beta} + E_i\,Q_i^{m\beta}\,.$$

In principle, we wish to determine $(R_i, E_i, s^\beta, c^\beta)$ which minimize the error:

$$\mathscr{E}^G = \sum_{\beta=1}^{N_\beta} \mathscr{E}^\beta\,,$$

$$\mathscr{E}^\beta \equiv \sum_{m=1}^{M} (s^\beta\,g_x^{m\beta} + c^\beta - g_0^{m\beta})^2$$

subject to the constraints of normalization:

$$\sum_{i=1}^{N_0} W_i\,R_i = 1, \quad \sum_{i=1}^{N_0} W_i\,E_i = 0\,,$$

which for Simpson rule weights $W_i\,(\frac{4}{3}h, \frac{2}{3}h, \frac{4}{3}h, \ldots)$ are equivalent to:

$$\int_{V_L}^{V_H} \mathrm{d}V\,\varrho\,(V) = 1, \quad \int_{V_L}^{V_H} \mathrm{d}V\,\xi\,(V) = 0\,.$$

The latter normalization, as pointed out earlier, fixes a scale on the unknown power parameter b.

It is well known that the solution of the above problem may be expected to show instabilities, worse as the "kernel" (P, Q) is smoother. This difficulty can be removed by a method due to Twomey [8], which amounts to adding to $\mathscr{E}^G$ terms which require the solutions (R, E) to be smooth in some sense, or to lie close to a given function. The addition of such terms may reduce the quality of fit; i.e., $(\mathscr{E}^G)_{\min}$ may increase, but normally this effect is very small while the solutions are greatly stabilized. In fact, in the ideal case, the loss of fit quality may well lie within the uncertainties in the given curves $g_x\,(\lambda, b^\beta)$, so that the added terms merely permit the choice of "reasonable" solutions from the class of solutions which fit the $g_x^{m\beta}$ to within their uncertainties. The amplitude of the smoothing parameter required will depend on the fraction of frequency range of the resonance curves used.

When $\mathscr{E}^\beta$ is expected, and optimization with respect to (s^β, c^β) is carried out, it has the form in matrix notation:

$$\mathscr{E}^\beta = R\,A^\beta\,\tilde{R} + 2\,R\,B^\beta\,\tilde{E} + E\,C^\beta\,\tilde{E}\,.$$

Smoothness can be imposed on R and E by adding to this error a term analagous to

$$\zeta \int_{V_L}^{V_H} \mathrm{d}V\,[\varrho''\,(V)]^2 \tag{3.4}$$

or

$$\zeta \int_{U_L}^{U_H} \mathrm{d}U\,[R''\,(U)]^2 \tag{3.5}$$

where ζ is a parameter which when increased, increases the smoothing effect. We have, in fact, added to $\mathscr{E}^G$:

$$(\zeta_1\,R\,A^R\,R + \zeta_2\,E\,A^E\,E)\,\mathrm{tr}\,(\sum_\beta A^\beta/N_0)$$

where

$$(A^R)_{ij} = (A^E)_{ij} = \left(\frac{U_i}{U_1}\right)^{N_p}\left(\frac{U_i}{U_1}\right)^{N_p} \cdot (6\,\delta_{|i-j|,0} - 4\,\delta_{|i-j|,1} + \delta_{|i-j|,2})\,.$$

Here the matrix is the second difference effect, $N_p = 0$ is analogous to (3.5), $N_p = 3$ is analogous to (3.4), and $\delta_{i,j}$ is the Kronecker delta. The trace is included for scaling purposes.

Furthermore, we have added:

$$\zeta_3\,E\,I\,\tilde{E}\,\mathrm{tr}\,(\sum_\beta A^\beta/N_0)$$

where I is the unit matrix; this permits us to make the individual values $E_i \to 0$ by choosing large ζ_3. (Note that the smoothness condition plus the normalization $W\tilde{E} = 0$ can also force $E_i \to 0$). If $\tilde{E}$ is to have the physical meaning of describing the effect of cavity window width, we must expect it to be small compared with R.

When in addition, a measured curve $\varrho_x\,(V)$ is available, we may require that R not differ much from $R_x \equiv V^2\varrho_x\,(V)$. Or, if the given curve $\varrho_x^w\,(V)$ has been generated by triangular windowing of the true (unknown) velocity distribution $\varrho_x\,(V)$,

$$R_x^w = w\,R_x\,\tilde{w}$$

we may require that $w\,R\,\tilde{w}$ not differ much from R_x^w too much. We have added then to $\mathscr{E}^G$ also:

$$(\zeta_4\,R\,A^\circ\,\tilde{R} + \zeta_5\,R\,A^w\,\tilde{R})\,\mathrm{tr}\,(\sum_\beta C^\beta/N_0)$$

where the matrices (A°, A^w) are easily derived errors from R_x and R_x^w. When ζ_4 is made sufficiently large (e.g. $\sim 10^4$), $R \to R_x$.

One further parameter is introduced. Since R is expected to provide a reasonably good fit even when $E = 0$, and since we must finally invert a matrix of dimension $[\dim(R) + \dim(E)]$, it is both desireable and practical to reduce the dimensionality of E to $N_E \leq N_0$. We define E^Γ of dimension N_E on equally spaced points $(U_0^E, U_1^E \ldots, U_{N_E+1}^E)$ where $U_0^E = U_L$ and $U_{N_E+1}^E = U_H$, taking $E_{N_E+1}^\Gamma = 0$, and assume $E\,(U)$ is adequately given by second-order spline interpolation of $E^\Gamma\,(U)$. This leads to an interpolation operator:

$$\tilde{E} = \Gamma\,\tilde{E}^\Gamma$$

which gives E when E^Γ is known.

Finally then, we determine (R, E) by minimizing over $(R, E^\Gamma, \eta_1, \eta_2)$ the complete quadratic form:

$$\begin{aligned}
&\mathscr{E}^T\,(R, E^\Gamma, \eta_1, \eta_2 \cdot b) \\
&= R\,(\sum_{\beta=1}^{N^\beta} A^\beta + \zeta_1\,A^R + \zeta_4\,A^\circ + \zeta_5\,A^w)\,R \\
&+ R\,(\sum_{\beta=1}^{N^\beta} B^\beta\,\Gamma)\,\tilde{E}^\Gamma \\
&+ E\,[\Gamma\,((\sum_{\beta=1}^{N^\beta} C^\beta) + \zeta_2\,A^E + \zeta_3\,I)\,\Gamma]\,E^\Gamma \\
&+ \eta_1\,(W\,\tilde{R} - 1) + \eta_2\,(W\,\Gamma)\,\tilde{E}^\Gamma
\end{aligned}$$

where (η_1, η_2) are Lagrange multipliers for normaliza-

tion terms. Note that $\zeta_4 = \zeta_5 = 0$ is to be taken when no experimental $\varrho_x(V)$ is used.

In the Program, DOPLR, R_0 is found first assuming $E^\Gamma = 0$ in $\mathscr{E}^T$ for comparison purposes, and then the full solution (R, E) is found. For both results, $(R_0, 0)$ and (R, E), (using $E = E^\Gamma \Gamma$), the rescaled fitting error:

$$e_m^\beta = g_x^{\beta m} - \left(\frac{g_0^{\beta m} - c^\beta}{s^\beta}\right),$$

and its rms value:

$$e_R^\beta = \left[\frac{1}{M}\sum_{m=1}^{M}(e_m^\beta)^2\right]^{\frac{1}{2}}$$

are computed. The e_R^β and its rms over β, e_R^T, are our principle diagnostic tools for evaluating the fitting quality for different values of the parameters involved.

IV. Applications

The method described in Section III has been applied to NBS-5 in two different geometries, and to a commercial beam tube. For simplicity, we shall discuss the results for the most recent NBS-5 alignment only.

Fig. 1 shows Ramsey resonance curves measured at (nearly optimum) power parameter b_0 (assumed unknown), at a 4 dB higher power level (b^+), and at a 6 dB lower power level (b^-), respectively. (b is proportional to the square root of the power). The minimum division on those graphs is 0.1 cm; the originals can be read to 0.05 cm, and the experimental error in the measurement should be less than this. We shall describe the fit of approximants to these resonance curves in centimeters.

Fig. 2 shows the velocity distribution $\varrho_x(V)$ (unnormalized) obtained by the pulse method using a velocity window of about $0.1 \cdot V$ ($r = 0.1$) [7].

We shall discuss first the determination of the distributions $[\varrho_0(V), \varrho(V), \xi(V)]$ obtained independent of knowledge of $\varrho_x(V)$, in order to show the effect of program parameters.

Outer bounds for velocity cutoffs may be estimated from, say, oven temperature, resonance half-widths, or ray-tracing. The estimates are not critical, as they can be improved by trial-and-error. We have taken $V_L = 100$ m/s, $V_H = 600$ m/s as initial estimates.

On each of the resonance curves, we have chosen $M = 22$ points equally spaced at frequency intervals of 5 Hz from the center (the first point at the center), spanning 105 Hz on one of the symmetric wings. (Any visible asymmetry in the curves is a warning that the theory used in this paper is inapplicable.)

We have used $N_p = 3$ for the velocity exponent in the smoothing operator to define more sharply the critical low velocity cutoff.

Figs. (3 and 4) show the resulting $\varrho_0(V)$ $[\xi(V)] \equiv 0)$ for $\zeta_1 = 10$ and $\zeta_1 = 10^3$ with $N_0 = 23$, $b_0 = 24000\ s^{-1}$. The instabilities for $\zeta_1 = 10$ are evident, while for $\zeta_1 = 10^3$, a very smooth curve is obtained. The rms fitting errors e_R^T are respectively 0.0846 and 0.1117 cm. These are too large to be consistent with the measurement accuracy of the resonance curves.

Retaining $\lambda_1 = 10^3$ to assure a stable solution, we swept b_0, obtaining the following errors:

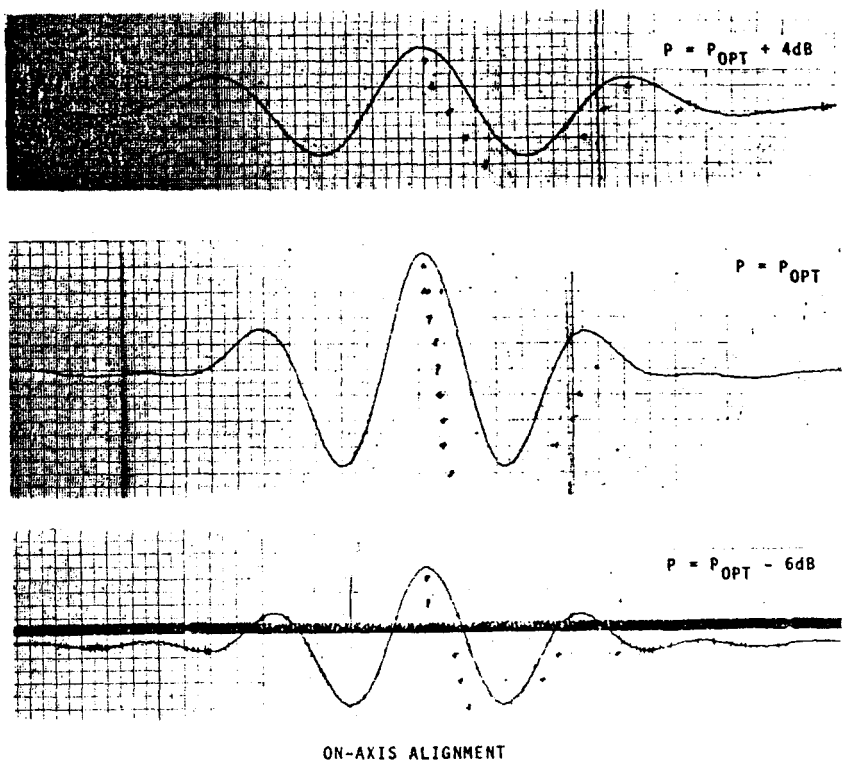

Fig. 1. Ramsey resonance records for NBS-5 on-axis alignment at nominally optimum power P_0, 4 dB above and 6 dB below. Finest division 0.1 cm. Calibration, 12.00 Hz/cm

$b_0 \cdot 10^{-4}$	e_R^T (cm)
2.2	0.0862
2.25	0.0788
2.3	0.0805
2.35	0.0920
2.4	0.1117

(4.1)

This gives a tentative best fit estimate of $b_0 = 22500\ s^{-1}$.

Fixing $b_0 = 22500\ s^{-1}$, other parameters remaining the same, we test for the correct low velocity cutoff V_L, with the following results:

V_L (m/s)	e_R^T (cm)
100	0.0788
140	0.0714
165	0.0712
175	0.0607
185	0.0613
190	0.0777
195	0.1044
200	0.1381

(4.2)

At first the fitting error decreases, as the estimating points for $\varrho_0(V)$ are concentrated more in the region of significant contribution, but after $V_L = 185$ m/s, the error rapidly increases, indicating that we are cutting off portions of the important velocity range. We fix a conservative cutoff at $V_L = 175$ m/s.

With that value for V_L, and with $b_0 = 22500\ s^{-1}$, the smoothing pressure ζ_1 with the following results:

ζ_1	e_R^T (cm)	Fig. No.
10^{-1}	0.0474	5
10^{0}	0.0481	6
10^{1}	0.0489	7
10^{2}	0.0509	8
10^{3}	0.0607	9

(4.3)

We note that the stability of the result rapidly improves as we move from $\zeta_1 = 10^{-1}$ to 10^2, the latter showing essentially no instability, while the fitting error changes slowly. At $\zeta_1 = 10^3$, the fitting error takes a significant jump, indicating that oversmoothing (loss of resolution in $\varrho(V)$] is occurring. For the remaining tests, we use $\zeta_1 = 10^2$ as a best compromise. (An earlier alignment of NBS-5 [9] has a two-humped velocity distribution, yet there was still a clear distinction between values of ζ_1 large enough to reduce the instability noise, but small enough to show the well-defined double hump.)

To test that for $V_L = 175$ m/s and $\zeta_1 = 10^2$, b_0 is still a near optimum estimate, we obtain the following results.

b_0/s	e_R^T
22000	0.0555
22500	0.0504
23000	0.0553

(4.4)

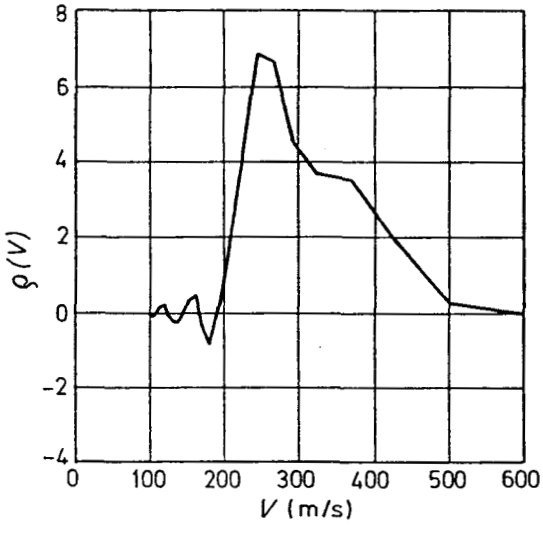

Fig. 3. Computed $\varrho(V)$, for $\xi(V) \equiv 0$, $N_0 = 23$, $b = 24000\ s^{-1}$, $\zeta_1 = 10$, $V_L = 100$ m/s, $V_H = 600$ m/s

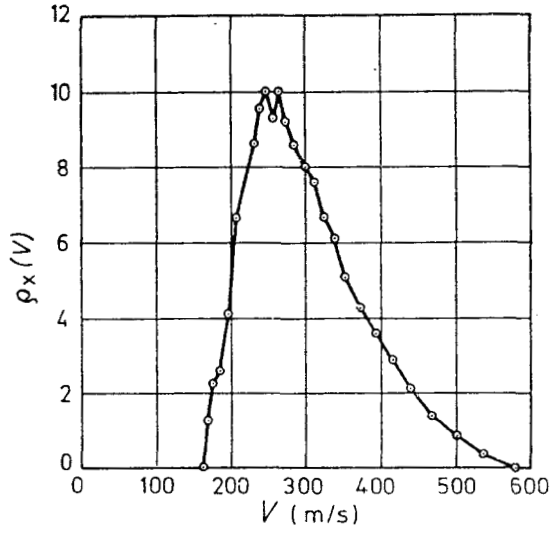

Fig. 2. Unnormalized velocity distribution for NBS-5 on-axis alignment obtained by pulse technique

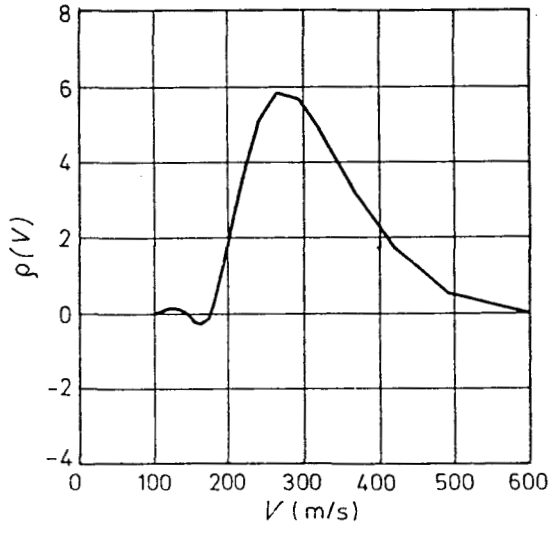

Fig. 4. Computed $\varrho(V)$ as in Fig. 3, but with $\zeta_1 = 10^3$, showing effect of smoothing parameter

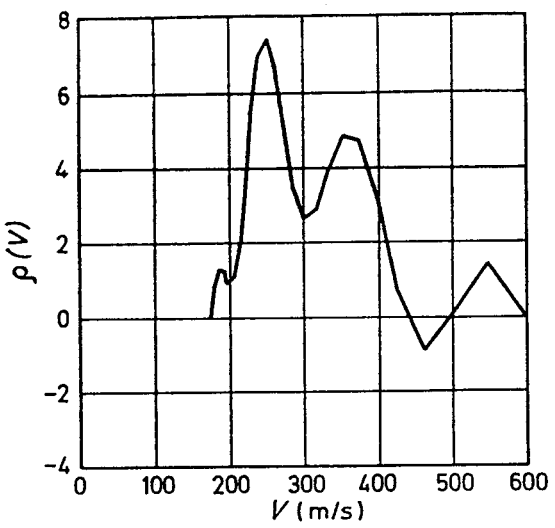

Fig. 5. Computed $\varrho(V)$, for $\xi(V) \equiv 0$, $N_0 = 23$, $b = 22500\ s^{-1}$, $V_L = 175$ m/s, $V_H = 600$ m/s, $\zeta_1 = 0.1$

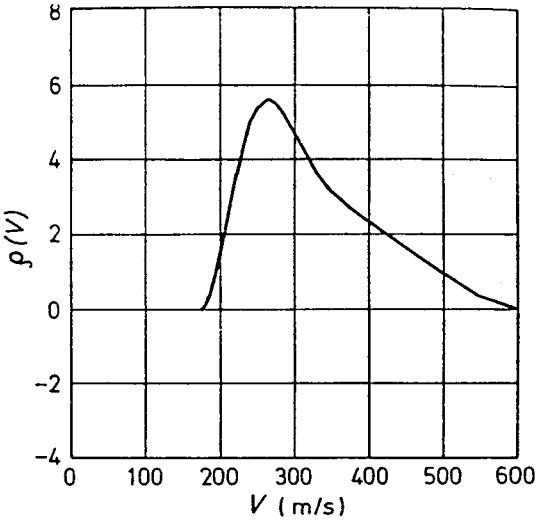

Fig. 8. As in Fig. 5, with $\zeta_1 = 10^2$

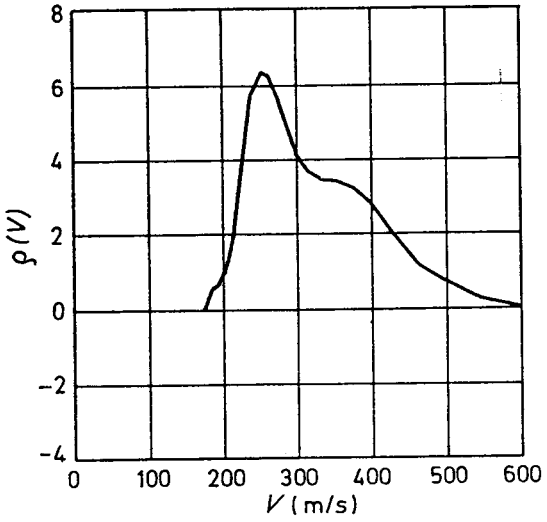

Fig. 6. As in Fig. 5, with $\zeta_1 = 1$

The influence of the number of velocity points N_0 is shown by the following, with $V_L = 175$ m/s, $b_0 = 22500\ s^{-1}$, $\zeta_1 = 10^2$:

N_0	e_R^T
19	0.0530
21	0.0515
23	0.0504

(4.5)

Thus $N_0 = 23$ seems to define $\varrho_0(V)$ in adequate detail. The estimate for b_0 is the same for these three cases to within $\Delta b = 50\ s^{-1}$. The distributions $\varrho_0(V)$ obtained for these cases are indistinguishable. That for $N_0 = 23$ is shown in Fig. 8.

The best estimate obtained to this point then $\varrho_0(V)$, $[\xi(V) = 0]$, for $V_L = 175$ m/s, $b_0 = 22500\ s^{-1}$ $\zeta_1 = 10^2$ (see Fig. 8), has $e_R^T = 0.0509$ cm. The worst errors (over m) to the three Ramsey curves are:

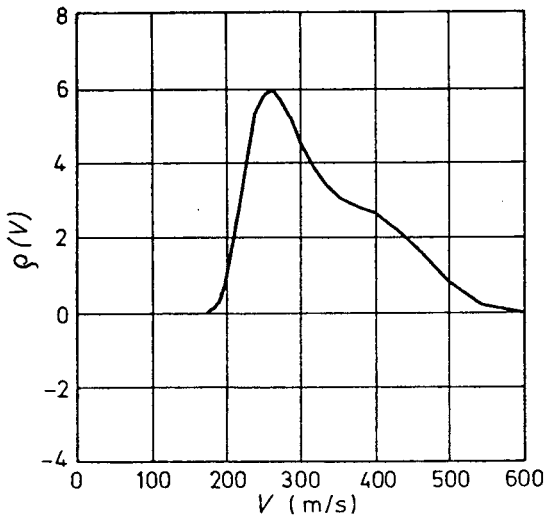

Fig. 7. As in Fig. 5, with $\zeta_1 = 10$

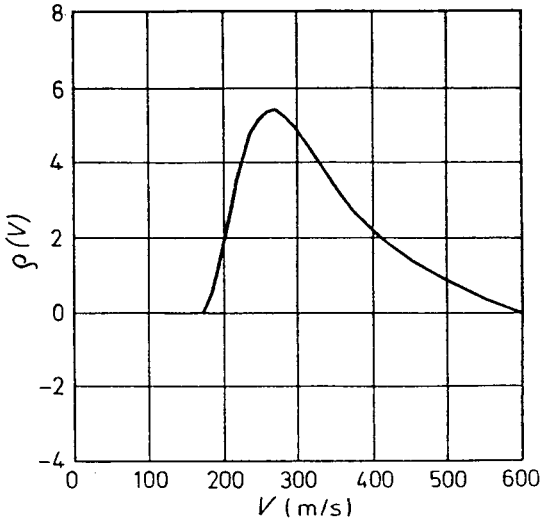

Fig. 9. As in Fig. 5, with $\zeta_1 = 10^3$

β	$(g_0^\beta - g_x^\beta)$ worst
1	—0.098
2	—0.089
3	+0.122

(4.6)

These errors still appear to be unacceptably large compared with the uncertainties in the measured values $g_x(\lambda, b^\beta)$.

On the other hand, if we accept the measured curve $\varrho_x(V)$, using the measured cutoff $V_L = 162.7$ m/s (V_H retained at 600 m/s), our program interpolates quadratically on $N_0 = 23$ intermediate points, $\varrho_I(V)$, shown in Fig. 10. Setting $\zeta^4 = 10^4$ caused the function $\varrho_I(V)$ to be reproduced as the solution (very high fitting-pressure). Minimum rms fitting error occurs for b_0 near 23000/s, as shown below:

b (s^{-1})	e_R^T
22500	0.2091
23000	0.1901
23500	0.1804
24000	0.1830

(4.7)

For $\varrho_I(V)$, we estimate $b_0 = 23640$ s^{-1}. This fitting error to resonance curves runs as high (over m) as 0.470 cm, which is much too large. Thus the distributions [$\varrho_I(V)$, $\xi(V) = 0$] are inconsistent with the measuren resonance curves. due presumably to measurement errors and windowing in $\varrho_x(V)$ and to a lesser extent the interpolation oi $\varrho_x(V)$ to $\varrho_I(V)$. As we shall see this inconsistency does not lead to large errors in bias estimation.

Having now established that, if $\xi \equiv 0$ then $V_L = 175$ m/s, $\lambda_1 = 10^2$, are near optimum parameters and lead to the best fit $\varrho_0(V)$ for $b_0 = 22500$/s, we shall examine what happens if $\xi(V)$ is obtained from $E(U)$, on spline interpolates of the N_E-point vector $E^\Gamma(U^\Gamma)$. Two questions should be answered. First, is $\xi(V)$ a significant addition to the analysis, or are we merely adding free parameters? Second, if $\xi(V)$ should in fact be included, does it significantly effect calculations of biases due to δ and DS, and hence the accuracy evaluation of the beam tube?

Toward the first question, we can contribute some affirming results for the NBS-5 study. Now $\xi(V)$ should, on the average, be small compared to $\varrho(V)$, so that λ_2 and λ_3 must be large enough to force this. In fact, we have taken λ_2 and $\lambda_3 = 0$, noting that the interpolation to N_E small already smoothes, and the results we obtain are already small enough to be acceptable.

Let us fix $V_L = 175$ m/s, $\lambda_1 = 10^2$, and examine the fitting errors while keeping the total number of free parameters $N_0 + N_E = 24$ fixed. However, for $\xi(V) \neq 0$, the optimum value of b_0 is affected, so that we must look also for best fits in b_0. We find for (N_0/N_E) values:

	b (s^{-1})	e_R^T (cm)
$N_0/N_E = 21/3$	23500	0.0262
	24000	0.0255
	24500	0.0378

(4.8)

from which we estimate $b_0 = 23780$:

	b (s^{-1})	e_R^T (cm)
$N_0/N_E = 19/5$	22500	0.0271
	23000	0.0258
	23500	0.0252

(4.9)

from which we estimate $b_0 = 23680$/s. These should be compared with results (4.4) for $N_0 = 23$, $N_E = 1$ ($\xi = 0$), and with (4.7) for the measured distribution.

For the $N_0/N_E = 21/3$ case, using $b_0 = 23780$/s, we find the worst fitting errors: $e_R^T = 0.0233$ cm.

β	$(g_0^\beta - g_x^\beta)$ worst (cm)
1	—0.035
2	+0.028
3	—0.062

(4.10)

While for 19/5, $b_0 = 23680$/s: $e_R^T = 0.0252$ cm.

β	$(g_0^\beta - g_x^\beta)$ worst (cm)
1	—0.035
2	+0.034
3	—0.066

(4.11)

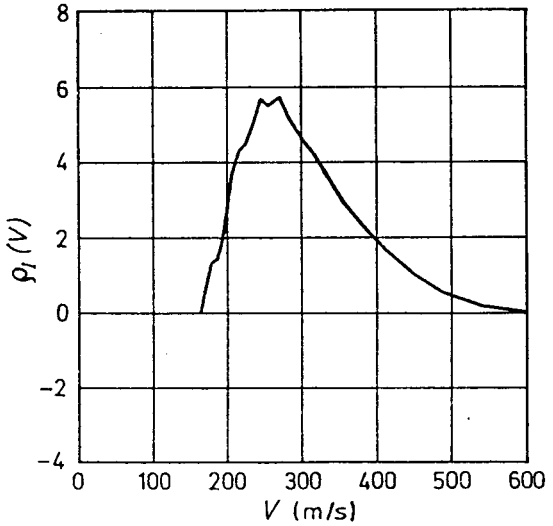

Fig. 10. Normalized $N_0 = 23$ quadratic interpolation $\varrho_I(V)$ of measured distribution of Fig. 2

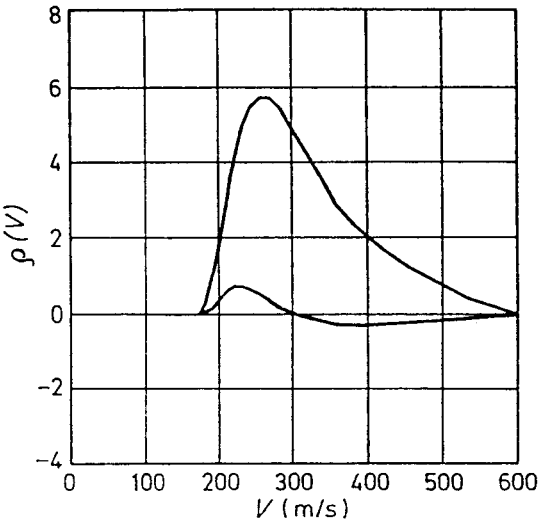

Fig. 11. Computed [$\varrho(V)$, $\xi(V)$], $N_0/N_E = 21/3$, $b_0 = 23780$ s^{-1}, $\zeta_I = 10^2$, $V_L = 175$ m/s, $V_H = 600$ m/s

These results should be compared to the results (4.6) for the 23/1 ($\xi = 0$) case.

The distributions (ϱ, ξ) are plotted in Figs. 11 and 12 for optimal b_0 for the cases N_0/N_E being 21/3 and 19/5 respectively. Clearly the curves $\xi(V)$ are substantially defined, and give a significant improvement to the resonance curve fit over the 23/1 ($\xi = 0$) case, which has an equal number of free parameters. The shape of the $\xi(V)$ curve is consistent with the view that slower atoms, which are deflected more in the focussing magnets, tend to lie closest to the window edges of the resonant cavities, where the field parameter reduction ϵ is largest.

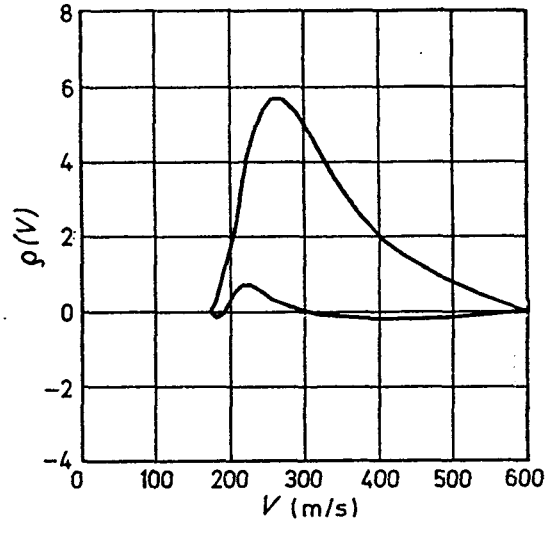

Fig. 12. Computed $[\varrho(V), \xi(V)]$, $N_0/N_E = 19/5$, $b_0 = 23680\ s^{-1}$, $\zeta_1 = 10^2$, $V_L = 175$ m/s, $V_H = 600$ m/s

We have shown that the addition of the second distribution $\xi(V)$ does substantially improve the fit of computed and generated resonance curves, and that the function is well-enough defined by N_E equal to 3 or 5 to reduce the fit error in the case we have studied to the level of measurement noise. We shall now discuss the second question: does the introduction of $\xi(V)$ significantly effect the accuracy figure obtained by bias measurements as described in Section II (B)?

We shall assume the frequency shift $\nu_C^+ - \nu_C^-$ is measured when the power is changed from the upper value (+4 dB) to the lower value (−6 dB), and neglect any error in the measured ratios:

$$b^+ : b_0 : b^- = 1.5850 : 1 : 0.8563.$$

Suppose, as a typical shift, we find:

$$\nu_C^+ - \nu_C^- = 3.0\ (10)^{-3}\ \text{Hz},$$

and that the modulation width is known to be (exactly) 20 Hz.

Results (4.12) are obtained for $\Delta^+ \equiv \nu_C^+ - \nu_0$ and δ when the $[\varrho(V), \xi(V), b_0]$ are assumed in the following cases:

Case 1: results (4.7), with $\varrho;(V)$, $\xi(V) = 0$, $b_0 = 23640\ s^{-1}$.

Case 2: results (4.6), with $\varrho_0(V)$, $\xi(V) = 0$, $b_0 = 22500\ s^{-1}$.

Case 3: results (4.8), with $\varrho(V)$, $\xi(V)$, $N/_0N_E = 21/3$, $b_0 = 23780\ s^{-1}$.

Case 4: results (4.9), with $\varrho(V)$, $\xi(V)$, $N_0/N_E = 19/5$, $b_0 = 23680\ s^{-1}$.

Case	Δ^+ (Hz)	δ (radians)
1	−0.00978	0.000277
2	−0.00823	0.000099
3	−0.00748	0.000031
4	−0.00754	0.000037

(4.12)

Finally, to answer the second question relative to the particular case discussed, for $\varrho_1(V)$ and the three distributions obtained for N_0/N_E of (23/1, 21/3, 19/5) at their respective best estimated for b_0, the bias differences all lie within 2.3 $(10)^{-13}$ of the cesium resonant frequency. The addition of the function $\xi(V)$ changes the bias by about 0.8 $(10)^{-13}$ as compared to the best estimate for $\varrho_0(V)$ with $\xi = 0$. Thus these refinements are important only if accuracy better than 1.0 $(10)^{-13}$ is required. (But see reference [10]).

Before we can consider the results obtained so far to be of practical value for bias estimates to the 10^{-13} level, it is important to consider the effect on the bias calculation when certain experimental and analytical parameters are uncertain. We shall restrict ourselves to the $N_0/N_E = 21/3$, $\zeta_1 = 10^2$, $V_L = 175$ m/s, $V_M = 600$ m/s which has given the best result for $N_0 + N_E = 24$ at $b_0 = 23780$/s [see Results (4.8), (4.10), and (4.12, case 3)]. We designate the resulting distributions for this case $[\varrho_N(V), \xi_N(V)]$ (see Fig. 11). They have been obtained assuming the Ramsey resonance curves were for power levels *precisely* 4 dB above and 6 dB below the nominal 0 dB level, i.e. at:

$$b^+ = 37689\ s^{-1}, \quad b^- = 11918\ s^{-1}.$$

The following table shows the results which would have been obtained using (ϱ_N, ξ_N) with varying values of the experimental parameters b^+, b^-, ν_{MOD}, $\nu^+ - \nu^-$:

b^+ (s^{-1})	b^- (s^{-1})	ν_{MOD}(Hz)
37689	11918	20
37689	11918	*21*
37689	11918	20
37689	*11782*	20
38125	11918	20

$\nu^+ - \nu^-$ (Hz)	Δ^+ (mHz)	δ (μrad)
−0.0030	−7.48	31.
−0.0030	−7.55	34.
−0.0031	−7.90	58.
−0.0030	−7.47	30.
−0.0030	−7.17	5.

(4.13)

The changes in the (b^+, b^-) are 0.1 dB power changes.

Results (4.13) show that, for this case, uncertainties in upper and lower power setting of 0.1 dB, in modulation width of 1 Hz, and in the power shift measurement of 0.1 mHz give maximum bias uncertainty (accuracy) of less than 0.8 mHz, or fractionally less than 0.8×10^{-13}. These levels of experimental control are considered feasible.

We now consider the effect of an error in the "power setting relative to optimum power" in the determination of (ϱ, ξ). We suppose that $g_x^{(2)}(\delta)$ corresponds to a +4.1 dB power level (instead of 4.0 dB as assumed above). Results corresponding to (4.8) are the following:

	b (s^{-1})	e_R^T (cm)	
$N_0/N_E = 21/3$	23000	0.0275	
(P of 4.1 dB)	23500	0.0243	(4.14)
	24000	0.0318	

from which we estimate $b_0 = 23400$ s^{-1}. Using $b_0 = 23400$ s^{-1}, we obtain the distributions $[\varrho_p(V), \xi_p(V)]$ which give fitting errors analagous to (4.10) $e_R^T = 0.0243$ cm.

β	$(g_0^\beta - g_x^\beta)$ worst (cm)	
1	—0.038	
2	—0.033	(4.15)
3	—0.061	

Corresponding to results (4.13), using (ϱ_p, ξ_p) leads to the following uncertainty table:

b^+ (s^{-1})	b^- (s^{-1})	ν_{MOD} (Hz)
37087	11728	20
37087	11728	*21*
37087	11728	20
37087	*11594*	20
37515	11728	20

(4.16)

$\nu^+ - \nu^-$ (Hz)	Δ^+ (mHz)	ζ (μrad)
—.0030	—7.85	62.
—.0030	—7.93	65.
—.0031	—8.28	90.
—.0030	—7.84	61.
—.0030	—7.52	24.

These curves (ϱ_p, ξ_p) are scarcely distinguishable from (ϱ_N, ξ_N) shown in Fig. 11. Referring to the first lines of (4.13, 4.16), we see that the 0.1 dB upper power level error leads to a bias change of less than 0.4 mHz. The incremental changes in the remainder of (4.16) are the same as in (4.13).

Finally, we check the effect of the smoothing parameter, using $\xi_1 = 10^1$ (slight undersmoothing, see Figs. 9, 10) instead of $\zeta_1 = 10^2$. Results corresponding to (4.8) are the following:

	b (s^{-1})	e_R^T (cm)	
$N_0/N_E = 21/3$:	23000	0.0279	
(ζ_1 at 10^1)	23500	0.0225	(4.17)
	24000	0.0231	

from which we estimate $b_0 = 23700$ s^{-1}. Using $b_0 = 23700$ s^{-1}, we obtain the distributions $[\varrho_\zeta(V), \xi_\zeta(V)]$, which give fitting errors analagous to (4.10):

$$e_R^T = 0.0218 \text{ cm}$$

β	$(g_0 - g_x^\beta)$ worst (cm)	
1	0.034	
2	0.029	(4.18)
3	—0.055	

Corresponding to results (4.13), using $(\varrho_\zeta, \xi_\zeta)$ leads to the following uncertainty table:

b^+ (s^{-1})	b^- (s^{-1})	ν_{MOD} (Hz)
37502	11878	20
37562	11878	*21*
37562	11878	20
37562	*11742*	20
37997	11878	20

(4.19)

$\nu^+ - \nu^-$ (Hz)	Δ^+ (mHz)	δ (μrad)
—0.0030	—7.58	38.
—0.0030	—7.65	41.
—0.0031	—8.00	65.
—0.0030	—7.57	37.
—0.0030	—7.26	11.

From the first lines of (4.13) and (4.19), we find the error in choosing the smoothing parameter ζ_1 distinguishing Figs. 7 and 8 is only 0.1 mHz. The figure sequence 5—9 and the e_R^T values of (4.3) fix the proper value of ζ_1 at least within a factor of 10. The incremental changes in the remainder of (4.19) are again essentially the same as in (4.13).

With those estimates, one can write the bias error budget estimate for DS and cavity phase difference.

Error Source		Error in Δ^+ (mHz)
1. Ramsey curve power level errors		
Upper level	0.03 dB	0.11
Lower level	0.03 dB	<0.01
2. Computing/parameter errors		
$N_E = 3$ to $N_E = 5$		<0.10
ϱ_1	factor of 10	0.10
Truncations		<0.10
3. Bias experiment errors		
Nominal power reset[1]	0.03 dB	.10
Upper level set	0.03 dB	.10
Lower level set	0.03 dB	< .01
ν_{MOD} error	1 Hz	.07
Shift Measurement ($\nu^+ - \nu^-$) error	0.1 mHz	0.42
Total		<1.03 mHz

The major source of uncertainty is the shift measurement itself. The above is, of course, for data relating to NBS-5. However, for other beam tubes we may expect no significant difference to this error analysis.

V. Conclusions

We have shown that the Ramsey resonance curves in atomic beam machines can be conceived as resulting from velocity-averaging of two distributions of velocity, $\varrho(V)$ and $\xi(V)$, with their respective transition probabilities, $P_0(\lambda, V, b, \delta)$ and $P_\in(\lambda, V, b, \delta)$ [see Eq. (2.12)].

An analysis and computer program are described which permit one to obtain $\varrho(V)$, $\xi(V)$, and a nominal power parameter b_0 from three (or more) carefully

[1] Ability to reproduce a previous power setting; e.g., the setting used in (1) above.

Table 1

q	L_q	K_q	M_q	N_q	q
1	0	$4S^2(1+3C^2)$	$8SC(2C\hat{S}+S\hat{C})$	0	0
2	al	$-16S^2C^2$	$-16SC(C\hat{S}+S\hat{C})$	$8\hat{a}lS^2C^2$	0
3	$2al$	$-4S^4$	$-8S^3\hat{S}$	$4\hat{a}lS^4$	0
4	$al+\lambda L$	$-8S^2C(1-C)$	$-4S[2C(1-C)\hat{S}+S(1-2C)\hat{C}]$	$4\hat{a}lS^2C(1-C)$	1
5	$al-\lambda L$	$8S^2C(1+C)$	$4S[2C(1+C)\hat{S}+S(1+2C)\hat{C}]$	$-4\hat{a}lS^2C(1+C)$	-1
6	$2al+\lambda L$	$-2S^2(1-C)^2$	$-2S(1-C)[(1-C)\hat{S}-S\hat{C}]$	$2\hat{a}lS^2(1-C)^2$	1
7	$2al-\lambda L$	$-2S^2(1+C)^2$	$-2S(1+C)[(1+C)\hat{S}+S\hat{C}]$	$2\hat{a}lS^2(1+C)^2$	-1
8	λL	$4S^2(1-3C^2)$	$4S(1-3C^2)S-12S^2C\hat{C}$	0	1

where $a=(\lambda^2+4b^2)$, $\hat{a}=4b^2/a$
$S=-2b/a$, $\hat{S}=S(1-\hat{a}/a)$
$C=-\lambda/a$, $\hat{C}=-C\hat{a}/a$

measured Ramsey resonance curves at power levels where ratios are known. The determination from the functions (ϱ, ξ) of bias errors due to second order Doppler shift, cavity phase difference and cavity pulling is described.

The methods are applied to the NBS-5 frequency standard. Error estimates indicate that it is feasible by microwave power shift measurements to evaluate the total bias error due to the above causes to within 1.0 MHz, or $1.(10)^{-13}\,\nu_0$.

VI. Acknowledgements. The author wishes to thank Helmut Hellwig for his valuable suggestions and encouragement.

Appendix

Calculation of the transition probability follows Ramsey's formulation ([6], V. 29 to V. 37, V. 44), except that in Eqs. V. 29 and V. 30 which refer to the first cavity, we use a_1 and Θ_1, (depending on b_1), while in Eq. V. 34, which refers to the second cavity, we use a_2 and Θ_2. We obtain analogous to V. 34:

$$C_q(2\tau+T)=\tfrac{1}{4}\sum(k_q+m_q e^{i(\lambda T+\delta)})e^{il\,q}$$

where the sum is over the four terms obtained from $s_1=\pm 1$, $s_2=\pm 1$, with

$$k_q=s_2\sin\theta_2(1+s_1\cos\theta_1)$$
$$m_q=s_1\sin\theta_1(1-s_2\cos\theta_2)$$
$$l_q=\tfrac{1}{2}\tau(s_1a_1+s_2a_2).$$

From this, the transition probability P is readily expressed as a weighted sum of cosines. Expanding this sum to first order terms in ϵ_1 and ϵ_2 leads directly to Eqs. (2.2, 2.3) with the coefficients of Table 1.

VII. References

1. Harrach, R. J.: J. Appl. Phys. 38, 1808 (1967)
2. Holloway, J. H., Lacey, R. F.: In: Proc. Colloque international de chronométrie, Lausanne, V. 1, 317 (1964)
3. Mungall, A. G.: Metrologia 7, 49 (1971)
4. Shirley, J. H.: J. Appl. Phys. 34, 788 (1963).
5. Hellwig, H., Barnes, J. A., Glaze, D. J., Kartaschoff, P.: U.S. Nat. Bur. Stand. Tech. Note 612 (1972)
6. Ramsey, N. F.: Molecular Beams, Oxford 1956
7. Hellwig, H., Jarvis, S., Glaze, D. J., Halford, D., Bell, H. E.: Time Domain Velocity Selection Modulation as a Tool to Evaluate Cesium Beam Tubes, 27th Ann. Freq. Contr. Symp. (to be published)
8. Twomey, S.: Monthly Weather Rev. 94, 363 (1966)
9. Glaze, D. J.: Recent Progress on the NBS Primary Frequency Standard, 27th Ann. Freq. Contr. Symp. (to be published)
10. If the bias measurement is made between the power levels +4 dB and 0 dB, however, the addition of the function $\xi(V)$ may make a difference of $3.(10)^{-13}$, because the coefficients V_D, V_P are rapidly changing near 0 dB.

USCOMM - ERL